Minimum Required Capture Radius in a Coplanar Model of the Aerial Combat Problem

John V. Breakwell*
Stanford University, Stanford, Calif.
and
Antony W. Merz†
Aerophysics Research Corporation, Mountain View, Calif.

Coplanar aerial combat is modeled with constant speeds and specified turn rates. The minimum capture radius which will always permit capture, regardless of the initial conditions, is calculated. This "critical" capture radius is also the maximum range which the evader can guarantee indefinitely if the initial range, for example, is large. A composite barrier is constructed which gives the boundary, at any heading, of relative positions for which the capture radius is less than critical.

I. Introduction

THE present differential-game model of the fixed-role, coplanar aerial combat problem considers the speeds and the maximum turn rates of the two aircraft to be given parameters, together with the pursuer's all-aspect weapon range, or "capture radius." When these parameters are sufficiently in favor of the pursuer, the evader can never avoid eventual capture, regardless of the initial conditions, if the pursuer maneuvers optimally. Otherwise, the evader can remain outside the capture circle from some initial conditions, if the proper evasive turn maneuvers are used in certain critical geometries.

The object of this analysis is to specify the minimum capture radius which will always permit capture, regardless of the initial conditions. This "critical" capture radius is clearly also the maximum range which the evader can guarantee indefinitely if the initial range, for example, is large.

II. Parameters and Equations of Relative Motion

As in the "Game of Two Cars"[1] the study requires the numerical specification of the speeds V_P and V_E and the maximum horizontal turn rates $\omega_{P_{\max}}$ and $\omega_{E_{\max}}$, where P and E denote pursuer and evader, respectively. Since only the *relative* performance is important, the parameters can be nondimensionalized for brevity, by normalizing with the pursuer's speed and maximum turn rate; i.e.,

$$\gamma = V_E / V_P < 1$$

$$\omega = \omega_{E_{\max}} / \omega_{P_{\max}}$$

The unit of distance in these normalized equations is the pursuer's minimum turn-radius, which usually varies considerably with flight condition, but is of the order of a mile for typical combat aircraft. The coplanar geometry is then as shown in Fig. 1, where the position of the evader relative to the pursuer is given by (x,y) in axes fixed to P. The relative heading is H, measured clockwise from P's velocity direction to E's velocity direction. The relative position can be expressed equivalently as range, $r=\sqrt{x^2+y^2}$ and bearing, $\varphi=\tan^{-1}(x/y)$.

Received Feb. 8, 1977; revision received April 26, 1977.
Index categories: Guidance and Control; Performance; Analytical and Numerical Methods.

*Professor of Astronautics. Fellow AIAA.

†Research Specialist. Member AIAA.

With these changes, the normalized equations of relative motion become

$$\dot{x} = -\omega_P y + \gamma \sin H \tag{1a}$$

$$\dot{y} = -1 + \omega_P x + \gamma \cos H \tag{1b}$$

$$\dot{H} = -\omega_P + \omega_E, \quad |\omega_P| \le 1, \quad |\omega_E| \le \omega \tag{1c}$$

III. Relevant Differential Game

We now suppose that, from any initial state (x, y, H), P seeks to minimize the ensuing minimum range and E to maximize it. Except for relatively trivial initial states such that E can cause the range to increase immediately, this is a game of "terminal payoff," the payoff being the value, say β, of the separation $r=\sqrt{x^2+y^2}$ at the first instant when $\dot{r}=0$. The critical nondimensional capture radius β_c is the value of β corresponding to optimal play from any sufficiently larger initial range. We remark in passing that, as Cockayne[2] has shown, if $\omega\gamma<1$, so that E's lateral acceleration is, like his velocity, less than P's, P can always achieve "point capture," i.e., $\beta_c=0$. To determine β when $\omega\gamma>1$ we must treat the game of terminal payoff in the usual way:

$$\min_{\omega_P} \max_{\omega_E} \{\mathcal{H} = V_x\dot{x} + V_y\dot{y} + V_H\dot{H}\} = 0 \tag{2}$$

where the adjoint variables V_x, V_y, V_H satisfy the differential equations

$$\dot{V}_x = -\partial\mathcal{H}/\partial x = -\omega_P V_y \tag{3a}$$

$$\dot{V}_y = +\omega_P V_x \tag{3b}$$

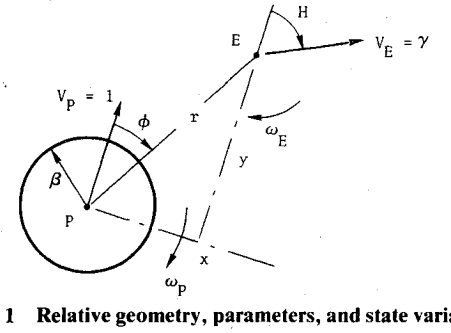

Fig. 1 Relative geometry, parameters, and state variables.

$$\dot{V}_H = -\gamma(V_x \cos H - V_y \sin H) \tag{3c}$$

and the terminal values

$$(V_x, V_y, V_H)_{t_f} = [(x/r), (y/r), 0]_{t_f} \tag{4}$$

Before proceeding further, we turn now to the limiting case $\omega = \infty$.

Critical Capture Radius When Evader's Turn Rate Is Infinite

The critical capture radius here corresponds to the largest closed barrier in Isaacs' Homicidal Chauffeur game, and is given by (9.1.4) of Ref. 1:

$$\beta_c = \gamma \sin^{-1}\gamma + \sqrt{1-\gamma^2} - 1 \tag{5}$$

provided that $\beta_c^2 + \gamma^2 \leqq 1$ (so that $\ddot{r}_f \geqq 0$), i.e., $\gamma \sin^{-1}\gamma \leqq 1$. We may verify Eq. (5) by observing that, as long as the range exceeds γ, P can keep E directly ahead, whatever E does. As the range decreases, E must choose the moment to break right or left, thereby optimizing the initial range y; the initial adjoint V_y is thus zero. But in this game ($\omega = \infty$) H becomes E's control; V_H remains zero; and E's velocity γ (sin$H$, cos$H$) is aligned with (V_x, V_y) which, as follows from (3), remains fixed in a nonrotating reference frame. E thus runs in a straight line to right or left in a direction perpendicular to the initial range vector. Since, according to Eq. (4), E's heading must coincide with his bearing from P at the instant when $\dot{r} = 0$, $H_f = \varphi_f = \cos^{-1}\gamma$ and the actual paths have the form shown in Fig. 2a. The distance traveled by E is $\gamma \sin^{-1}\gamma$ and relation (5) is verified easily.

A different analysis is necessary if $\gamma \sin^{-1}\gamma > 1$. The terminal condition in this case is one of "equilibrium,"[3] at which $\dot{x}_f = \dot{y}_f = 0$, with $\varphi_f > \cos^{-1}\gamma$ and $H_f > \varphi_f$. In this terminal configuration, P and E are describing concentric circles of radii 1 and γ, at the same angular rate, and the equilibrium heading relates the final range to the speed ratio by the law of cosines:

$$\beta_c^2 = 1 + \gamma^2 - 2\gamma \cos H_{eq}$$

At minimum range, E has moved through unit distance in the time $1/\gamma$, and P therefore has turned through the angle $1/\gamma$.

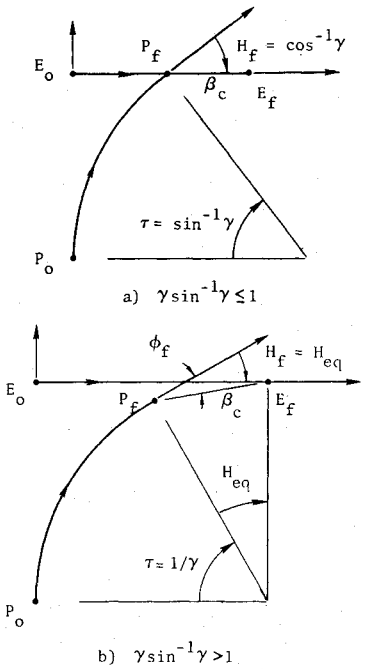

Fig. 2 Critical trajectories when evader's turn rate is infinite.

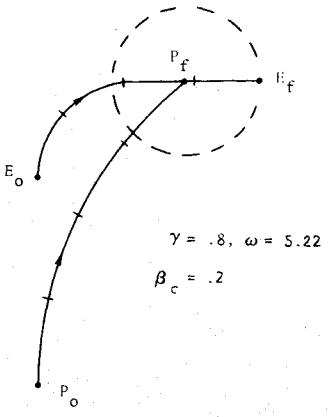

Fig. 3 Critical trajectories in region I.

Consequently, as shown in Fig. 2b, $H_{eq} = \pi/2 - 1/\gamma$ and

$$\beta_c = \sqrt{1 + \gamma^2 - 2\gamma \sin(1/\gamma)} \tag{6}$$

Modifications Due to Evader's Finite Turn Rate

The distance lost by the evader because of his finite turn rate is $R_B(\pi/2 - 1)$, where $R_B = \gamma/\omega$ is E's minimum turn radius as he turns toward his optimal direction which is again normal to the initial relative velocity. In fact $\omega_E = \omega \operatorname{sgn} V_H$, and (sin$H$, cos$H$) parallel to (V_x, V_y) now defines a singular arc with $\omega_E = 0$ toward which E turns. A representative near-miss maneuver is shown in real space in Fig. 3, and the generalization of Eq. (5) is seen to be

$$\beta_c = \gamma \sin^{-1}\gamma + \sqrt{1-\gamma^2} - 1 - (\gamma/\omega)[(\pi/2) - 1] \tag{7}$$

In applying this formula, the speed ratio must satisfy the inequality $\gamma \geqq \sin(\pi/2\omega)$, since E's speed and turn rate must be high enough to permit a 90° turn before minimum range is reached. The region of parameter space (γ, ω) for which $\gamma \geqq \sin(\pi/2\omega)$, and $\gamma \sin^{-1}\gamma \leqq 1 + (\gamma/\omega)[(\pi/2) - 1]$, so that $\beta_c^2 + \gamma^2 \leqq 1$, will be referred to as region I, and (7) is the corresponding critical capture radius.

The trajectories in Fig. 3 are shown for the speed ratio $\gamma = 0.8$ and a capture radius $\beta_c = 0.2$, and E's turn rate then is computed using Eq. (7), giving $\omega = 3.22$. It may be noted that the pursuer is always turning at maximum rate, whereas E's optimal path ends with a straight path or singular arc. At the time of minimum range, P is turning toward E, and E is moving directly away from P. At the beginning of these optimal maneuvers, however, P is leading (turning away from) E, while E is turning toward P's future trajectory. Both

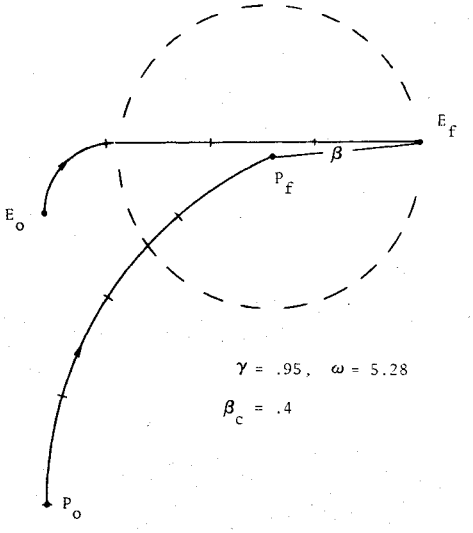

Fig. 4 Critical trajectories in region II.

of the paths have been broken into four equal subarcs, and it is seen that E crosses P's velocity vector when the paths are about 60% completed. After this time P is lagging E, as expected. The evader delays his turn to left or right as long as possible to prevent P from leading him prematurely.

A similar modification of (6) is necessary for $\omega<\infty$, in a region II of parameter space defined by $\gamma \geqq \sin(\pi/2\omega)$ and $\gamma \sin^{-1}\gamma \geqq 1+(\gamma/\omega)[(\pi/2)-1]$. When E must turn through 90° before reaching the equilibrium heading, the extra maneuver time is proportional to the extra distance covered by E in turning toward the final heading. It follows that P must turn for an additional time equal to $(\pi/2-1)/\omega$, and the generalization of Eq. (6) is therefore

$$\beta_c=\sqrt{1+\gamma^2-2\gamma \sin[1/\gamma+(\pi/2-1)/\omega]} \tag{8}$$

As before, E's final heading is slightly *greater* than the final bearing. The trajectories in Fig. 4 have been shown for the parametric values $\beta_c=0.4$, $\gamma=0.95$, and $\omega=5.28$, as computed by Eq. (8). These parametric values have been chosen so as to make the geometry easier to follow and are not meant to be representative of any actual pair of aircraft.

A third region, III, of parameter space distinct from the foregoing corresponds to an evader only slightly more maneuverable than the pursuer, the parameters then satisfying the inequalities

$$1/\omega \leq \gamma \leq \sin(\pi/2\omega) < 1$$

For such parameters, minimum range occurs while E is still turning toward his optimal direction, and the following equations are satisfied:

$$\beta_c+1-\cos\tau=(\gamma/\omega)(1-\cos\omega\tau) \tag{9a}$$

$$\sin\tau=\gamma\sin\omega\tau \tag{9b}$$

These equations can be derived by noting that P turns through the angle τ while E turns through $\omega\tau$, that $\dot{r}_f=0$, and that the final real-space range vector from P to E is (as in the first case) normal to the initial range vector. This can be seen in Fig. 5, where the paths of pursuer and evader are shown for the parameters $\gamma=0.9$, $\omega=1.25$, for which Eq. (9) gives $\beta_c=0.034$. As in Figs. 3 and 4, both trajectories are marked at three intermediate times, and in this case E crosses P's velocity vector very near the end of the turns.

IV. Variation of Critical Capture Radius with Speed and Turn Rate Parameters

The interdependence of the critical capture radius β_c, the speed ratio γ, and the maximum turn rate ratio ω is shown in Fig. 6, which is a graphical version of Eqs. (7-9), in their respective regions of parameter space. (An entirely equivalent analysis has been carried out by Sharma and Miloh, not yet published.) For practical applicability, the figure is drawn only for speed ratios in the interval from 0.5 to 1. The three regions are separated by dashed lines, and it is seen that the open-barrier condition can be guaranteed for *any* value of the evader's turn rate if the capture radius exceeds the value $\beta_{\max}=\sqrt{2(1-\sin 1)}\cong 0.563$. Smaller values of β_c are needed to guarantee capture as V_E decreases below V_P or as $\omega_{E_{\max}}$ decreases from infinity.

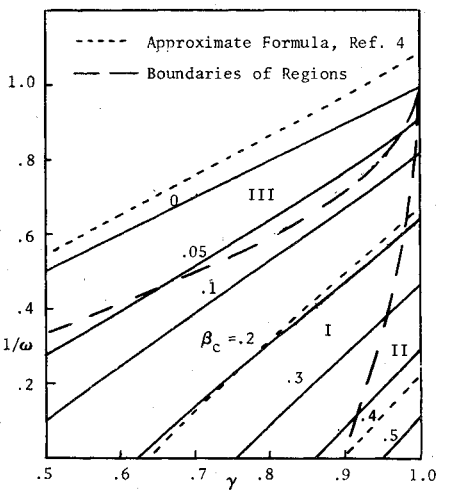

Fig. 6 Variation with speeds and turn rates of minimum required capture radius.

The parameter space has been labeled in three major regions, corresponding to the three types of terminal geometries discussed in Sec. III. That is, tail-chase trajectories for parameters from region I will have the form shown in Fig. 3, whereas those for regions II and III will have the forms pictured in Figs. 4 and 5.

Kelley and Lefton[4] give a crude approximate formula for β_c which turns out to be reasonably accurate in all three regions. The contours of constant β_c corresponding to this formula are included in Fig. 6 for β_c equal to 0, 0.2, and 0.4.

V. Barrier in State Space (x,y,H) Corresponding to $\beta=\beta_c$

The largest closed barrier in Isaacs' Homicidal Chauffeur game is clearly the boundary of the region of initial states (x,y) for which $\beta<\beta_c$. A similar barrier must exist in state space (x,y,H) when ω is finite, and we turn now to its construction.

We start, following Isaacs, by backward construction of the paths of the game described in Sec. III. In regions I and III the barrier paths terminate at the critical range $r_f=\beta_c$, and the minimum range condition is $\dot{r}_f=-\cos\varphi_f+\gamma\cos(H_f-\varphi_f)=0$. This expression relates the final heading ambiguously to the final bearing; i.e.,

$$H_f=\varphi_f\pm\cos^{-1}\left[\frac{\cos\varphi_f}{\gamma}\right]$$

which implies that the terminal bearing must satisfy $|\varphi_f|\geq\cos^{-1}\gamma$.

Restricting attention to positive terminal bearings (i.e., at minimum range, E is to the *right* of P's velocity vector), P is turning hard right toward E at minimum range, regardless of E's final relative heading. The slower evader should be turning away from P at minimum range, and the range-rate equation shows that, if the final heading satisfies $-\cos^{-1}\gamma<H_f<\cos^{-1}\gamma$, E should be turning hard right at this time. On the other hand, if the heading falls in the open interval $\cos^{-1}\gamma<H_f<2\pi-\cos^{-1}\gamma$, E should be turning hard left at minimum range. In both cases, E is turning away from P. If $H_f=-\cos^{-1}\gamma$, E's velocity is directed at P, and at such a "dispersal point," E can turn optimally either way; $\omega_E=\pm\omega$. However, if $H_f=\cos^{-1}\gamma$, E's velocity is radially outward, E is on a singular arc, and $\omega_E=0$, both at termination and for

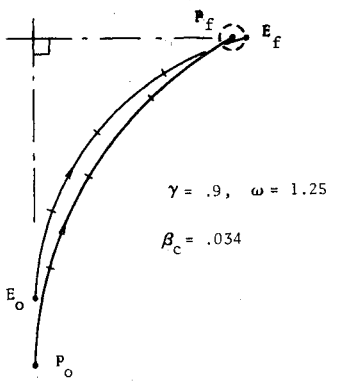

Fig. 5 Critical trajectories in region III.

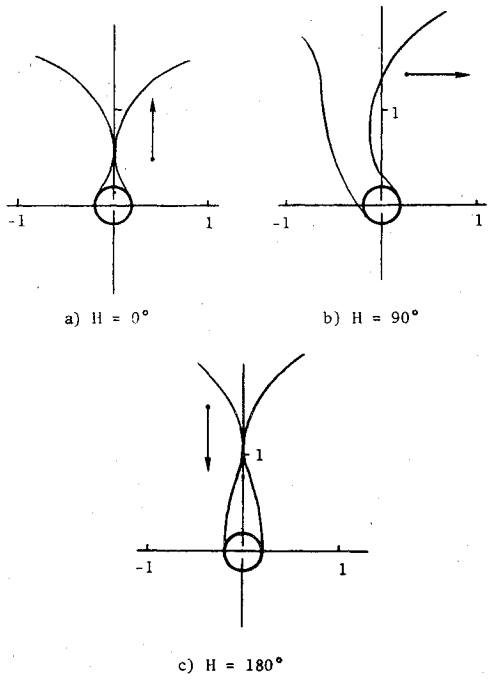

Fig. 7 Appearance of barrier for parameters in region I.

an interval prior to termination. All of these optimal terminal maneuvers are intuitively correct, in a physical sense.

The appearance of the barrier surface can be found as suggested by Isaacs (Ref. 1, p. 243) by fixing the relative heading and then calculating the right and left barrier coordinates (x,y) corresponding to the appropriate maneuver combinations. Thus, e.g., the right barrier will be composed of relative paths corresponding to the maneuvers P_RE_R, P_RE_{RS}, P_RE_L, and P_RE_{LS}, where R, L, and S abbreviate right, left, and straight (singular arc) maneuvers for P and E. For parameters in regions I and III the results are qualitatively as shown in Fig. 9.2.3 of Ref. 1, and a quantitative plot of a barrier is shown in Fig. 7 at the headings $H=0$, 90°, and 180° for the region I parameters $\gamma=0.8$, $\omega=3.22$, $\beta_c=0.2$. Notice that the barriers close tangentially at $H=0°$ and 180°, but that they are *open* for $H=90°$. This question is addressed in Sec. VI.

If the evader's maximum turn rate is increased, the parameters move from region I to region II of parameter space. Here the equilibrium point exists, as illustrated in Fig. 4, and the "barely closed" barrier takes a slightly different form. Specifically, the orientation of the terminal adjoint vector no longer varies smoothly with position on the capture circle along the minimum range locus, $\dot{r}_f=0$. Instead, the terminal adjoint vector is directed radially outward when the heading exceeds the equilibrium heading,

$$H_{eq}=\cos^{-1}\left[\frac{1+\gamma^2-\beta^2}{2\gamma}\right] \tag{10}$$

This vector, however, is not radially outward when the terminal heading equals H_{eq}, when E is ahead of P. It follows that the barrier normal is discontinuous across the trajectory (P_RE_L) which ends at H_{eq}, and a ridge or crest occurs across this line on the barrier surface.

For headings less than H_{eq}, the barrier trajectories are qualitatively different from those which occur in regions I and III, since now the terminal heading is always equal to H_{eq}. That is, E's optimal maneuvers are, in order, $\omega_E=\omega$, 0, and 1, while P turns right with $\omega_P=1$. The resulting barrier surface does not always end on the capture circle at the locus $\dot{r}_f=0$, and a typical appearance of the barrier near H_{eq} is shown in Fig. 8.

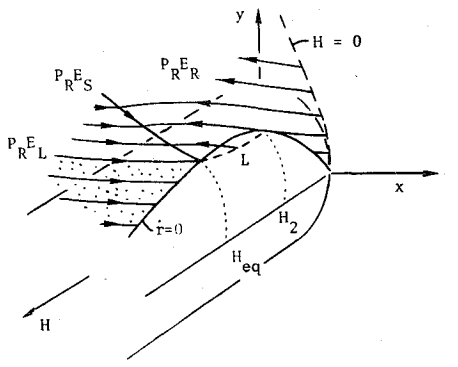

Fig. 8 Appearance of barrier near equilibrium point.

The construction of the barrier was made easier by the realization that the radial acceleration is *negative* when $r_f=\beta$, $\dot{r}_f=0$ for headings in the angular interval $H_1<H_f<H_{eq}$, where H_1 is the root to the radial acceleration equation, $\ddot{r}_f(H_f)=0$. This means that the locus $\dot{r}_f=0$ does *not* denote the end of the barrier in this angular range, since trajectories can arrive at this locus only from *inside* the capture circle. At the heading H_2 which is smaller than H_1, the barrier path from the locus L (indicated in Fig. 8) leaves the capture circle tangentially, since here the locus L has rejoined the locus $\dot{r}_f=0$. The heading H_2 satisfies the equations which result when a two-part trajectory ending at the equilibrium point originates on the capture circle at the locus $\dot{r}_f=0$.

VI. Closing the Barrier

The barrier which has been constructed in the previous section just closes ahead of P at $H=0$, and at $H=\pi$, as shown in Fig. 7. This same barrier is actually *open* at other headings, as shown in Fig. 7 for $H=90°$. This means that the tail-chase and head-on geometries are desirable from E's point of view, because here E can prevent P from knowing which way to turn in order to lead E. The barrier at headings other than 0 or π can be closed by finding those positions from which E can barely return to the collinear geometry ($H=0°$ or 180°) before it is "too late." These positions are the start of a preliminary game terminating with $V_y>0$ at the coordinates

$$x_1=0, \qquad y_1=\gamma-\gamma/\omega, \qquad H_1=0$$

for the tail-chase geometry, or

$$x_2=0, \qquad y_2=\gamma+\gamma/\omega, \qquad H_2=\pi$$

for the head-on geometry. The composite final barrier will ultimately include only the closer of these two barrier segments, as will be shown in Fig. 9. During the preliminary game E simply turns toward the heading $H=0$ or $H=\pi$, as the case may be. P's strategy is more complex and requires detailed analysis as follows. The adjoint histories during this preliminary game must satisfy Eq. (3) and are thus expressible as:

$$V_x=K\cos\beta\sin(\alpha+\omega_P\tau)$$

$$V_y=K\cos\beta\cos(\alpha+\omega_P\tau)$$

$$V_H=K\{\sin\beta-(\gamma/\omega_E)\cos\beta[\cos(\alpha+\omega_E\tau-H_f)-\cos(\alpha-H_f)]\}$$

where H_f is 0 or π, τ is time-to-go in this preliminary game, and K and the angles α, β are constants which may be assumed to satisfy the inequalities: $K>0$, $\cos\alpha>0$, $\cos\beta>0$.

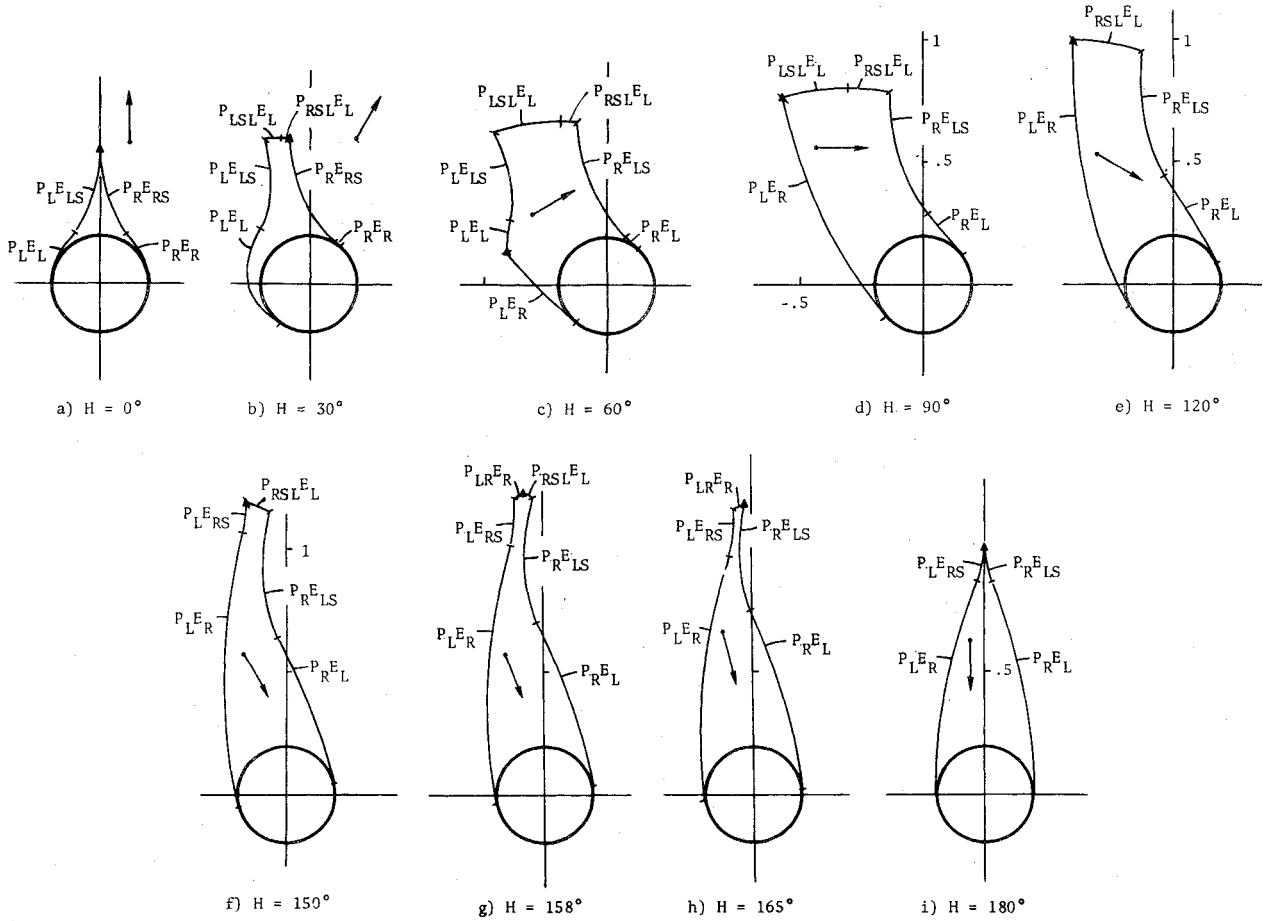

Fig. 9 Complete barrier in region I.

The vanishing of the Hamiltonian $\mathcal{H}$ leads to

$$\tan\beta = \frac{\gamma}{\omega}\sin\alpha + \frac{\gamma-1}{\omega-1}\cos\alpha, \qquad (H_f=0)$$

and

$$\tan\beta = \frac{1}{\omega-1}\left[\left(\gamma+\frac{\gamma}{\omega}\right)\sin\alpha + (\gamma+1)\cos\alpha\right], \quad (H_f=\pi)$$

P has a retrograde switch time τ_1 at which

$$S_P = yV_x - xV_y + V_H = 0$$

and hence

$$\tan\alpha = \frac{(1-\omega)\cos\tau_1 - \gamma + \omega}{(\omega-1)(\gamma+\sin\tau_1)} > 0, \qquad (H_f=0)$$

and

$$\tan\alpha = \frac{(\omega-1)\cos\tau_1 - \gamma - \omega}{(\omega+1)\gamma + (\omega-1)\sin\tau_1} < 0, \quad (H_f=\pi)$$

The switch time τ_1 can take values from 0 to τ^* where $dS_P(\tau)/d\tau$ vanishes at the same time τ^* as S_P. Hence τ^* is the first-quadrant solution of

$$\gamma\sin\tau^* + \frac{\gamma-\omega}{\omega-1}\cos\tau^* + 1 = 0, \qquad (H_f=0)$$

or

$$\gamma\sin\tau^* - \frac{\gamma+\omega}{\omega+1}\cos\tau^* + \frac{\omega-1}{\omega+1} = 0, \quad (H_f=\pi)$$

If $\tau=\tau^*$ the preceding path may be a singular arc for P along which $\omega_P=0$, and this singular arc may itself be preceded by a turn in either direction, $\omega_P=\pm 1$.

Representative barrier cross sections are shown at several headings in Fig. 9, for a set of parameters chosen in region I of Fig. 6, and previously illustrated in Fig. 3. The computed sectional views of this three-dimensional surface show clearly how the differential-game capture region varies with H for the parameters $\gamma=0.8$, $\beta_c=0.2$, and $\omega=3.22$. As with all such critical barrier surfaces, E can evade P indefinitely if E is initially *outside* the barrier. Likewise, P can capture E in finite time, regardless of E's evasive maneuvers, if E is initially *inside* the barrier; and, in general, both P and E can encounter singular arcs (straight dashes) on the barrier trajectories. The corners in Fig. 9 marked with triangles (▲) denote edges of the composite three-dimensional barrier which are "dispersive," in that the trajectories move away from the edge in a direction chosen by E. The unmarked corners correspond to trajectories which follow the edge. Bernhard[5] has discussed the conditions under which two single semipermeable surfaces can join to form a composite semipermeable surface. He requires that the optimal paths either do not approach the edge from either side, or, if they do, they do so either tangentially or with a switch on arrival, so as not to cross the edge. Our edges clearly meet his conditions (see also Ref. 1, p. 267).

Initial conditions on the near-horizontal barrier segment (for H less than about 158°) require P to follow a turn-straight-turn tactic as E turns hard in one direction before arriving at the tail-chase geometry. The tail-chase then requires P to turn hard toward E who follows a turn-straight tactic as shown in Fig. 3. At the heading $H=158°$, a dispersal point for E is shown at the top of the barrier, and here E can choose to turn either right (to the head-on configuration) or

left (to the tail-chase geometry). For headings greater than about 158°, the barrier segment which closes the capture region involves left-right turn maneuvers for P as E turns hard toward the head-on geometry, after which E again turns through 90° before encountering the singular arc.

Conclusions

The capture-radius required to guarantee capture in coplanar motion of a slower but more maneuverable evader has been found as a function of the speeds and maximum turn rates of the two aircraft. If the actual capture radius of the pursuer is less than the critical value required, the barrier is *closed,* the capture region is finite, and the evader can avoid capture indefinitely, if the evader is initially outside the capture region. Conversely, if the capture radius is larger than the critical minimum value required, the barrier is *open* and escape is impossible providing only that the pursuer maneuvers correctly.

The "barely closed" barrier which has been derived and discussed in this paper can be composed of surprisingly complex maneuvers, particularly when the pursuer is only slightly faster than the evader. The barrier has been illustrated for several ratios of aircraft speeds and turn rates, and both the form of the barrier and the associated maneuvers could be of practical interest to both designers and pilots of combat aircraft.

The duration of the encounter is in every case comparable with the short time taken by the pursuer to turn through a right angle. Since longitudinal accelerations are typically much smaller than normal accelerations, the assumption of constant speeds is not too unrealistic.

Acknowledgment

This research was carried out with NASA funding under contract NAS 2-9223.

References

[1] Isaacs, R., *Differential Games,* Wiley, New York, 1965.

[2] Cockayne, E., "Plane Pursuit with Curvature Constraints," *SIAM Journal of Applied Mathematics,* Vol. 15, Nov. 1967, pp. 1511-1516.

[3] Merz, A. W., "The Homicidal Chauffeur: A Differential Game," Stanford University, TR SUDAAR 418, March 1971.

[4] Kelley, H. J. and Lefton, L., "Estimation of Weapon-Radius vs Maneuverability Tradeoff for Air-to-Air Combat," *AIAA Journal,* Vol. 15, Feb. 1977, pp. 145-148.

[5] Bernhard, P., "Conditions de Coin pour les Jeux Differentiels," *Seminaire sur les Jeux Differentiels,* 1971, Centre d'Automatique, Paris.